Asian Journal of Chemistry; Vol. 26, No. 19 (2014), 6425-6430

ASIAN JOURNAL OF CHEMISTRY

http://dx.doi.org/10.14233/ajchem.2014.16414

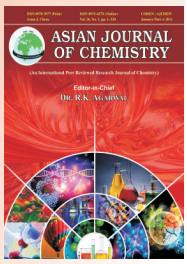

Effect of Vanadium Modification on Electrochemical Performance of $LiFePO_4$/C

YING ZHANG[1,2], JIANJUN SONG[1,2], GUANGJIE SHAO[1,2,*], ZHIPENG MA[1,2] and GUILING WANG[2]

[1]State Key Laboratory of Metastable Materials Science and Technology, Yanshan University, Qinhuangdao 066004, P.R. China
[2]Hebei Key Laboratory of Applied Chemistry, College of Environmental and Chemical Engineering, Yanshan University, Qinhuangdao 066004, P.R. China

*Corresponding author: Tel/Fax: +86 335 8061569; E-mail: shaoguangjie@ysu.edu.cn

Received: 24 September 2013; *Accepted*: 20 February 2014; *Published online*: 16 September 2014; AJC-15932

A series of vanadium doped $LiFePO_4$/C were synthesized by the carbothermal reduction method combining with balling technique. Results show that only a little of vanadium substitutes for iron site in the crystal lattice of olivine $LiFePO_4$ and impurity phases are detected when the vanadium content is over 0.5 mol %. $LiVOPO_4$, the first impurity phase, is discovered as vanadium content ranges from 1 mol to 5 mol % and disappears at high doping level. $Li_3V_2(PO_4)_3$ and vanadium oxide are gained when vanadium content is over 5 mol %. The special charge/discharge capacity and rate capability are enhanced on a certain extent by vanadium doping and $LiFe_{0.975}V_{0.025}PO_4$ shows the most outstanding property among all samples. The improvement of electrochemical performance of $LiFePO_4$ mainly resulted from the formation of impurity phases, $LiVOPO_4$, instead of the vanadium doping into $LiFePO_4$ lattice. Thus, excellent electrochemical performance can be achieved by optimizing the content of vanadium.

Keywords: $LiFePO_4$, Composites, Vanadium doping, X-ray diffraction, Impurity phase.

INTRODUCTION

Increasing attention is shown to $LiFePO_4$ as the next-generation cathode material in lithium-ion batteries due to its non-toxicity, safety, stability, high capacity and the abundance of raw materials[1]. But its low electrical (electronic and ionic) conductivity limits the electrochemical properties according to the charge/discharge rate capacity and operating temperature[2]. Decreasing particle size[3,4], doping supervalence-ion[5,6] and surface modification[7,8] are the most normal and efficacious way to overcome the weakness. Among these approaches, doping supervalence-ion is a convenient and effective way to improve the electrochemical performance of $LiFePO_4$.

Vanadium is a particularly attractive element to be considered for modifying the $LiFePO_4$, because it might substitute on the Fe site forming a VO_6 group[9] or on the tetrahedral P site forming a VO_4^{3-} group[10] and it exists over a wide range of oxidation state forming various electrochemical active vanadium compounds, such as V_2O_5[11], VO_2[12], V_2O_3[13], $LiVPO_4F$[14], $LiVOPO_4$[15], $Li_3V_2(PO_4)_3$[16], which can join in the process of Li^+ insertion and desertion. Sun *et al.*[9] confirmed with Rietveld refinement that V-ion substituted Fe-ion in the $LiFePO_4$ matrix structure and the improvement of electrochemical property definitely owed to the vanadium doping. Omenya *et al.*[16] reported that excessive vanadium could form impurity phase, $Li_3V_2(PO_4)_3$, at high doping level and the solid-solution limit depended on the preparation method and heat-treatment temperature. Besides $Li_3V_2(PO_4)_3$, other impurities are also discovered. Zhang *et al.*[17] found that two impurity phases co-existed, $Li_3V_2(PO_4)_3$ and $LiVOPO_4$, when vanadium content ranged from 5 mol to 10 mol %. Ma *et al.*[12] discovered that the state and compound of vanadium changed with the doping level. V^{4+} substituted for Fe ($LiFe_{1-x}V_xPO_4$, $0 < x < 0.07$) within the solid solubility, VO_2 distributed on the surface of the V-doped $LiFePO_4$ beyond the solid-solution limit and the formation of the secondary phase $Li_3V_2(PO_4)_3$ coexisted with the V-doped $LiFePO_4$ when vanadium content was over 11 mol %. Jin *et al.*[13] stated that vanadium did not step into the crystal lattice and the improvement of electrochemical performance for the cathode eventually resulted from the co-coating of carbon and V_2O_3.

In this work, a series of vanadium doping $LiFePO_4$/C were synthesized with different levels. We demonstrated the existence of two impurity phases by XRD. Moreover, we researched the influence of vanadium compounds on electrochemical performance of $LiFePO_4$ and discuss the major factor on enhancing the electrochemical performance in our paper.

EXPERIMENTAL

Iron oxide (Fe_2O_3), lithium dihydrogen phosphate (LiH_2PO_4) and vanadium pentoxide (V_2O_5) with Li:Fe:V:P molar ratios of 1:1-x:x:1 (x = 0, 0.005, 0.01, 0.015, 0.025,

0.05, 0.1) were mixed with citric acid through a planetary balling process for 5 h, followed by heat-treatment at 700 °C for 12 h under pure nitrogen to obtain $LiFe_{1-x}V_xPO_4$. Excessive citric acid (5 wt %) as the carbon source was mixed with precursors by balling for 5 h. Subsequently, the mixtures were heated at 700 °C for 10 h in N_2 and the carbon coated $LiFe_{1-x}V_xPO_4$ were synthesized.

The crystallographic structural characterization was analyzed by X-ray diffraction (XRD, Rigaku D/max-2500/pc, CuK radiation) and X-ray photoelectron spectroscopy (XPS, Thermo Escalab 250, Al Kα). The particle morphology and surface texture of samples were observed with field-emission scanning electron microscope (FE-SEM, S-4800).

The electrochemical performance of $LiFe_{(1-x)}V_xPO_4$/C cathode material was evaluated using columnar simulation cells. Active material powder (80 wt %) was mixed with acetylene black (10 wt %) and poly (vinylidene fluoride) binder (10 wt %) in N-methy1-2-pyrrolidone (NMP) to obtain slurry. The slurry was coated onto an aluminum foil and dried under vacuum at 120 °C for 12 h. Finally, the laminate was cut into round discs (1 cm in diameter) to be used as the working electrode. The electrolyte was 1 mol L^{-1} $LiPF_6$ dissolved in the mixture of ethylene carbonate (EC) and diethyl carbonate (DMC) with ratio of 1:1. Histogram cells were assembled in the glove box filled with argon gas. Charge-discharge tests were conducted on a battery test system (CT2001A, LAND, China) with cut-off voltages of 2.4 and 4.2 V (*vs.* Li/Li^+) at different current rates at room temperature. Cyclic voltammetry (CV) measurements were performed on an electrochemical working station (LK2005, LANLIKE, China) at a slow scanning rate of 0.1 mV s^{-1} within a voltage range of 2.4-4.2 V. And the electrochemical impedance spectroscopy (EIS) was employed to characterize the interfacial resistance of cathode using a Chenh ua CHI660A electrochemical workstation over the frequency range from 1 MHz to 0.01 Hz with amplitude of 10 mV ms^{-1} at room temperature.

RESULTS AND DISCUSSION

X-ray diffraction patterns of the as-prepared samples with different vanadium contents in the range of 0-10 mol % are shown in Fig. 1. It is revealed that the composition phases in $LiFe_{(1-x)}V_xPO_4$/C samples vary with the vanadium content. All diffraction peaks of pristine $LiFePO_4$/C powders and $LiFe_{(1-x)}V_xPO_4$/C with low vanadium content (x = 0.005) can be indexed with an ordered orthorhombic $LiFePO_4$ phase (Pnmb). No visible difference can be detected between the XRD patterns of two samples, indicating that V had doped into the host lattice. Impurity phase is formed when the vanadium content is over the solid solution limit and the peaks of $Li_3V_2(PO_4)_3$ are distinctly detected in the high level vanadium-doped $LiFePO_4$/C samples ($x \geq 0.05$). But another impurity appears before the presence of $Li_3V_2(PO_4)_3$, which could be the lithium vanadium oxide or lithium vanadium phosphate and it disappear when the vanadium is over 5 mol % (Fig. 1b). Comparing the diffraction peaks of the impurity phase with the standard PDF card, it could be $LiVOPO_4$. The result reveals that only little of vanadium step into the lattice and the formation of vanadium impurity changes with the doping level.

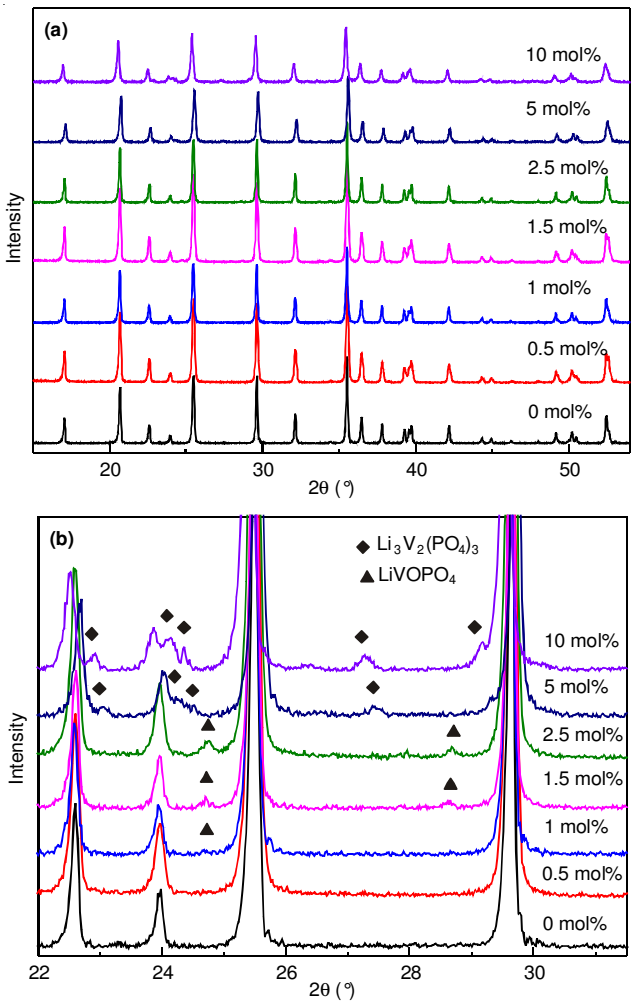

Fig. 1. XRD patterns of $LiFe_{(1-x)}V_xPO_4$/C (x = 0, 0.005, 0.01, 0.015, 0.025, 0.05, 0.1)

To prove our statement in further step, the selected $LiFe_{(1-x)}V_xPO_4$ (x = 0.025, 0.05, 0.1) samples were dissolved by dilute hydrochloric acid, washed with deionized water and dried under vacuum to obtain the remainders. Fig. 2 shows the XRD patterns of the remainders which could be consisted of carbon and vanadium oxide. According to our analysis, the XRD patterns don't match to a certain compound, indicating that a series of complicated vanadium oxides coexist in the acid lysates. Although the composition can't be known definitely, the patterns can help us to conclude whether the same vanadium composition is formed in the selected samples. Compared with peaks of lysates, the components in sample a (x = 0.025) are different from sample b and c (x = 0.05, 0.1), demonstrating that the vanadium composition in $LiFe_{0.975}V_{0.025}PO_4$/C is different from the one in $LiFe_{0.95}V_{0.05}PO_4$/C and $LiFe_{0.9}V_{0.1}PO_4$/C, consistent to our former opinion. It is still not solved that why the vanadium phase is changed with the content. It is possible that the formation of $Li_3V_2(PO_4)_3$ needs a stated vanadium content and energy. When the vanadium content doesn't reach the level or the surface energy is too high to obtain, an intermediate product, $LiVOPO_4$, is formed and it transforms into $Li_3V_2(PO_4)_3$ when the condition is proper. The structure transformation of $LiVOPO_4$ to $Li_3V_2(PO_4)_3$ is successfully carried out by Kuo *et al.*[18]. The possible reaction mechanism is listed as follow[19]:

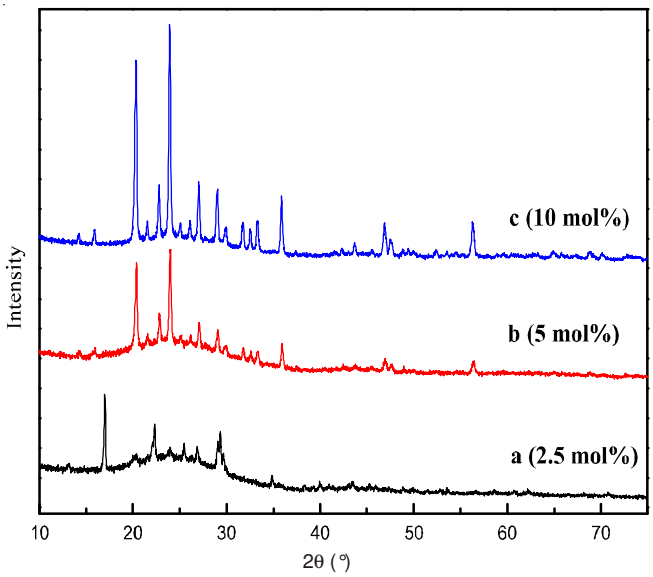

Fig. 2. XRD patterns of acid hydrolysis lystates from $LiFe_{(1-x)}V_xPO_4$ (x = 0.025, 0.05, 0.1)

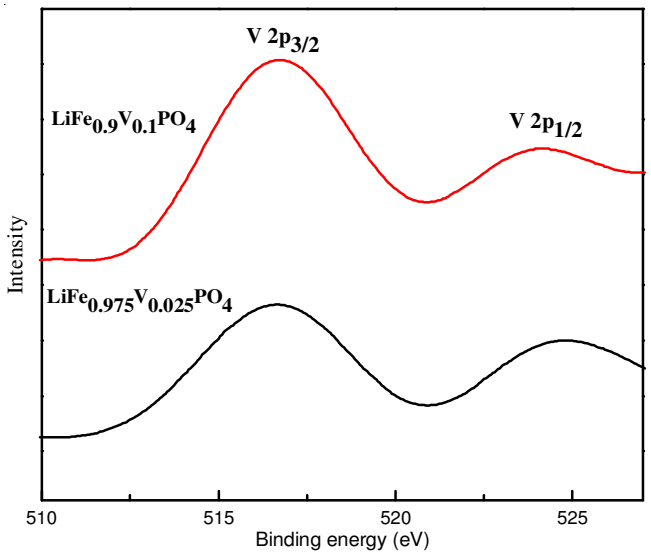

Fig. 3. XPS core level of V 2p for $LiFe_{0.975}V_{0.025}PO_4$ and $LiFe_{0.9}V_{0.1}PO_4$

$$3LiVOPO_4 \longrightarrow Li_3V_2(PO_4)_3 + VO_2 + 1/2\ O_2 \quad (1)$$

The selected samples were applied by XPS to ensure the valence and state of vanadium in the $LiFe_{(1-x)}V_xPO_4$/C, which is shown in Fig. 3. The typical two-peak structure of V 2p XPS spectra are V $2p_{3/2}$ peak and V $2p_{1/2}$ peak. Compared the binding energy values of V $2p_{3/2}$ and V $2p_{1/2}$ in the two samples with the standard ones, the valences of vanadium in the two samples are both between 3^+ - 4^+, which means that V^{3+} and V^{4+} co-exist in the material. The presence of V^{4+} in the $LiFe_{0.975}V_{0.025}PO_4$ is due to $LiVOPO_4$. And the V^{4+} in $LiFe_{0.9}V_{0.1}PO_4$ maybe originate from kinds of vanadium composition with high valence and could not be analyzed by XRD, such as VO_2, gained by the decomposition of $LiVOPO_4$. They cannot be detected by XRD because of their low content and poor crystallization.

Fig. 4 is the FE-SEM images of the $LiFe_{(1-x)}V_xPO_4$ (x = 0, 0.025, 0.05, 0.1). Low level vanadium doping doesn't make apparent change on the morphology of $LiFePO_4$, that is to say, vanadium doping and the formation of $LiVOPO_4$ don't influence the crystal growing direction.

Electrochemical performance: The galvanostatic discharge curves measured at 1 C for $LiFe_{(1-x)}V_xPO_4$ samples are shown in Fig. 5. The first discharge capacity is enhanced by doping and vanadium content is found to have a dramatic effect on the capacity. V substitutes for Fe and locates into the crystal lattice when the vanadium content is low, which is beneficial to improve the electrochemical performance, as the first discharge capacity of $LiFePO_4$/C and $LiFe_{0.995}V_{0.005}PO_4$/C are 124.6 and 132.8 mAh g^{-1}, respectively. Impurity phases present by increasing the vanadium doping level and the different phase has different effect on the capacity ability. According to the result of XRD, $LiVOPO_4$ is formed when the vanadium content is below 5 mol % and $LiFe_{0.975}V_{0.025}PO_4$ shows excellent performance, whose first discharge capacity is up to 166.3 mAh g^{-1}. When the vanadium content is over 5 mol %, a secondary phase, $Li_3V_2(PO_4)_3$, appears and $LiVOPO_4$ absents. As seen in Fig. 5, not only a discharge plateaus at 3.35 V for intercalation of Li^+ into $LiFePO_4$ but also three typical discharge plateaus around 3.57, 3.65 and 4.02 V for intercalation of two Li^+ reversibly into $Li_3V_2(PO_4)_3$ based on the V^{3+}/V^{4+} redox couple are distinctly observed in curves of the $LiFe_{0.95}V_{0.05}PO_4$/C and $LiFe_{0.9}V_{0.1}PO_4$/C, which matches well with the charge/discharge profiles of $Li_3V_2(PO_4)_3$/$LiFePO_4$ composites. The first discharge capacity of $LiFe_{0.95}V_{0.05}PO_4$/C and $LiFe_{0.9}V_{0.1}PO_4$/C are 158.4 and 136.1 mAh g^{-1}, respectively. Obviously, $LiVOPO_4$ is more efficient than $Li_3V_2(PO_4)_3$ to the improvement of electrochemistry performance of $LiFePO_4$. Because of the long heat-treating time and high

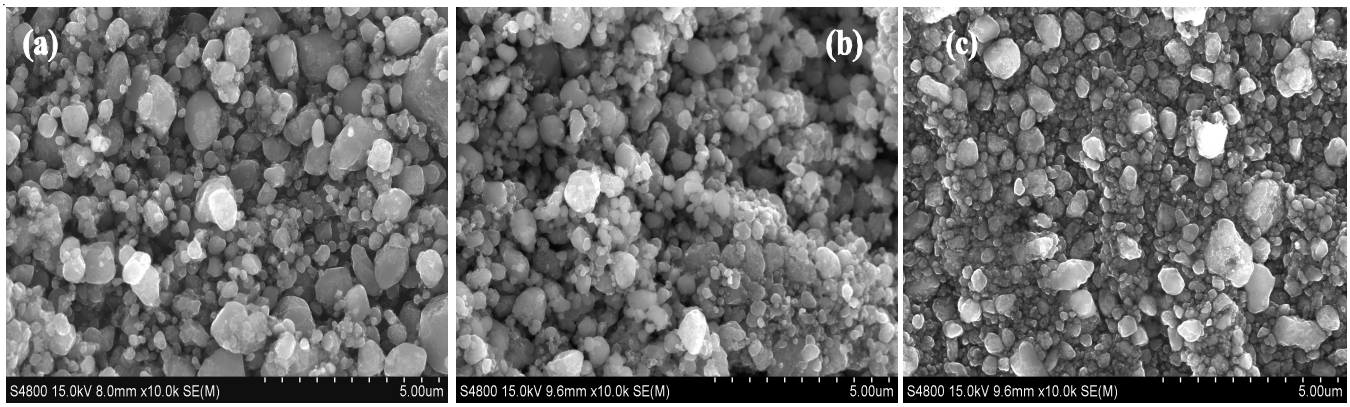

Fig. 4. SEM images of $LiFePO_4$/C (a), $LiFe_{0.975}V_{0.025}PO_4$/C (b) and $LiFe_{0.95}V_{0.05}PO_4$/C (c)

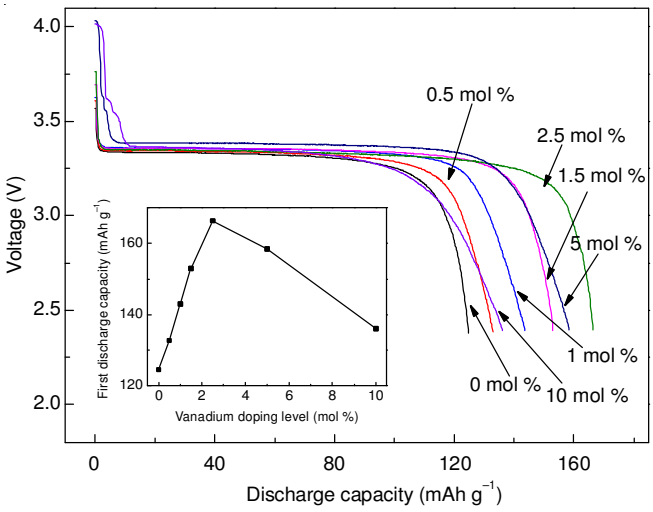

Fig. 5. Relationship between first discharge capacity and voltage measured at 1C for $LiFe_{(1-x)}V_xPO_4$ (x = 0, 0.005, 0.01, 0.015, 0.025, 0.05, 0.1)

temperature, the solid-solution concentration is low and the impurity phases appear when the vanadium is only over 0.5 mol %. Thus, it can be concluded that the enhancement of the electrochemical performance should be mainly due to the existence of a small amount of impurity phase, especially $LiVOPO_4$, rather than the doping of V in the host lattice.

To analyze the cyclic performance of the electrodes, selected samples are measured at different C rates and the results are shown in Fig. 6. The vanadium doped $LiFePO_4$ samples (2.5, 5 mol %) show better rate capacity than the pristine, especially at high C rate (5 C, 10 C). The transport of electrons from the particle surface to the current collector is the critical step, particularly at high current rate[20]. And the vanadium composition can improve the graphite degree of carbon to increase the electron transportation. Thus, the promotion is obvious at high rate, owing to the effect of impurity phase on the electron transport on the particle surface. Although $LiFe_{0.975}V_{0.025}PO_4$ still has an advantage over $LiFe_{0.95}V_{0.05}PO_4$ at high rates, the discharge capacity of $LiFe_{0.975}V_{0.025}PO_4$ goes downhill, due to the poor cyclic performance of $LiVOPO_4$.

Cyclo-voltammogram profiles reflect not only the electrochemical properties of the active material but also the electrochemical activity of the entire electrode. The cycle

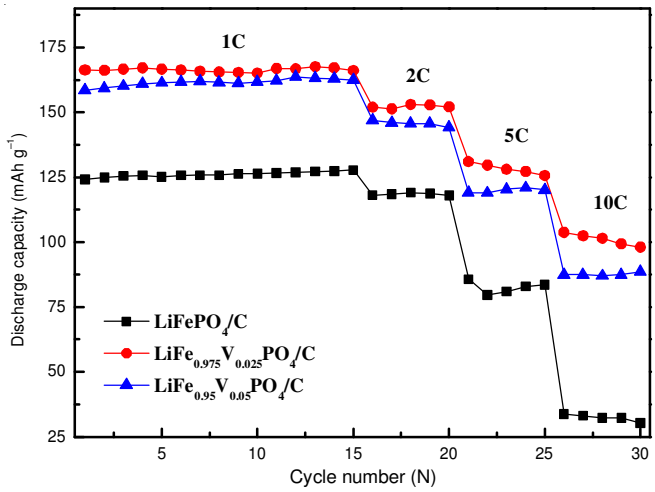

Fig. 6. Cycling performance of $LiFe_{(1-x)}V_xPO_4$ measured from 1C to 10C

voltammograms for the selected samples with a scanning rate of 0.1 mA s^{-1} are shown in Fig. 7. Only one couple of anodic and cathodic peaks, corresponding to the phase transition process of $LiFePO_4$ and $FePO_4$, are observed in the CV profiles of the pristine $LiFePO_4$/C and the $LiFe_{0.975}V_{0.025}PO_4$/C (Fig. 7a). Because of the low content of $LiVOPO_4$ in $LiFe_{0.975}V_{0.025}PO_4$/C, no anodic or cathodic peak of Li^+ extraction/insertion reaction in $LiVOPO_4$ is found in the curve. With an increase in the vanadium concentration to 5 mol %, three additional reduction peaks, associating with reduction potentials of $Li_3V_2(PO_4)_3$, are detected in Fig. 7b. Compared with other samples, especially the pristine, $LiFe_{0.975}V_{0.025}PO_4$/C shows a higher peaks intensity and a smaller difference between the reduction and oxidation potentials (0.205 V), indicating that the electrode reaction has a higher rate constant and a better reversibility of the Li^+ extraction/insertion reactions. This is the reason why $LiFe_{0.975}V_{0.025}PO_4$/C has the most excellent electrochemical property.

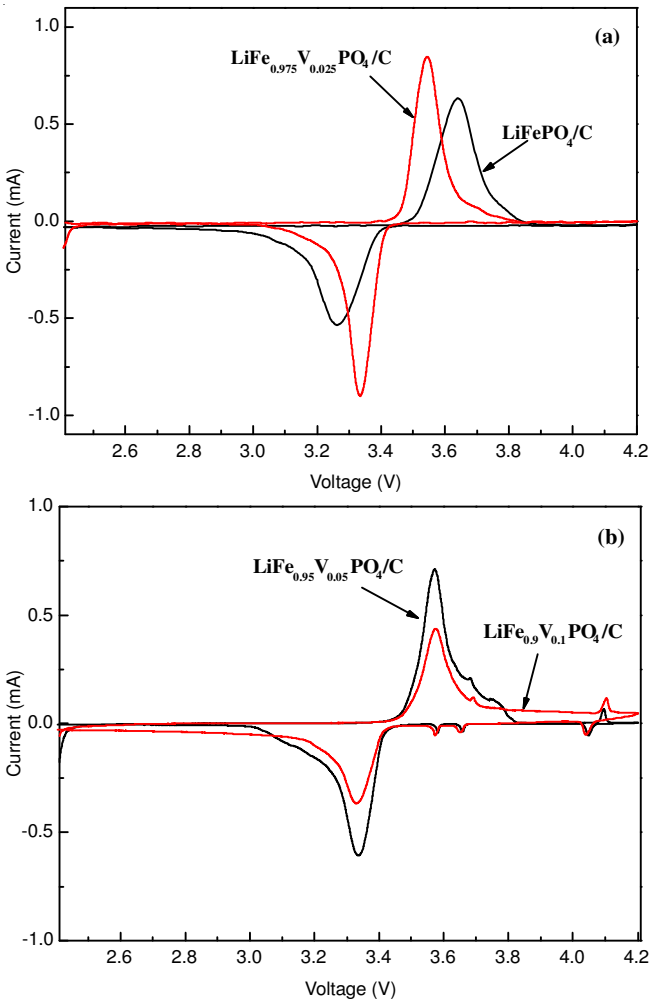

Fig. 7. CV profiles of $LiFe_{(1-x)}V_xPO_4$ at the scanning rate of 0.1 mA s^{-1} and in a potential window of 2.4-4.2 V (*vs.* Li^+/Li)

Fig. 8 shows the electrochemical impedance spectra (EIS) of the $LiFePO_4$/C and vanadium doped $LiFePO_4$/C electrode material after 5th cycle. EIS curves are composed of a depressed semicircle in high frequency region and a straight line in low frequency region. An intercept at the Z_{re} axis in the high frequency region corresponds to the ohmic resistance of

the electrolyte, followed by a semicircle in the middle frequency range, indicating the charge transfer resistance and a straight line in the low frequency region, related to the Warburg impedance due to the diffusion of the lithium-ion in the bulk of the electrode material. The impedance spectra can be described by the equivalent circuit presented in the inset picture, where R_s represents ohmic resistance, R_{ct} represents the charge transfer resistance, Z_w represents the Warburg impedance and the constant phase element CPE is placed to represent the double layer capacitance and passivation film capacitance[21]. The fitting results were analyzed by Zview-Impedance 2.80 software and R_{ct} values are listed in Table-1. The charge transfer resistance is related to complex reaction of charge transfer process between the electrolyte and the active materials[22]. Compared with the pristine, the impedance obviously decreases in the charge/discharge process with the appropriate amount of vanadium doping. The smaller charge transfer resistance indicates that lithium-ion and electron transfer are more feasible on the electrode and V-doping and impurity phases are benefit to overcome the restriction of kinetics in the charge/discharge process and improve the electrochemical activity of the material. But the improvement isn't continuous with the increasing vanadium doping level. The value of R_{ct} increases when vanadium content is over 2.5 mol %, which is consistent with the results of charge/discharge testing.

TABLE-1
IMPEDANCE PARAMETERS OF SAMPLES

Sample	$R_{ct}(\Omega)$	$j^0(mAg^{-1})$
$LiFePO_4$/C	927.8	27.7
$LiFe_{0.98}V_{0.015}PO_4$/C	559.5	45.9
$LiFe_{0.975}V_{0.025}PO_4$/C	264.5	97.1
$LiFe_{0.95}V_{0.05}PO_4$/C	470.3	54.6
$LiFe_{0.9}V_{0.1}PO_4$/C	804.7	31.9

The exchange current density (j^0) is a very important parameter of kinetics for electrochemical reaction and can measure the catalytic activity of electrodes. It is calculated using the following formula:

$$j^0 = R \cdot T / n \cdot m \cdot R_{ct} \cdot F$$

where R is the gas constant (8.314 J mol^{-1} K^{-1}), T is the temperature (298 K), n is the charge transfer number per molecule during the intercalation which is 1 for $LiFePO_4$, m is the mass of active material and F is the Faraday's constant (96,500 C mol^{-1}). The results are listed in Table-1 and the $LiFe_{0.975}V_{0.025}PO_4$/C exhibits a higher j^0, 97.1 *vs.* 27.7 mAh g^{-1}, than pure $LiFePO_4$/C, implying that the catalytic activity and the reversibility of $LiFe_{0.975}V_{0.025}PO_4$/C electrode are improved by doping V. The improvement of electrochemical performance of electrodes results from the existence of impurity phases which accelerate the catalytic activity and electron transfer on the particle surface. And $LiVOPO_4$, as a impurity phase, shows more prominent influence on the charge/discharge capacity, compared with $Li_3V_2(PO_4)_3$. The EIS results indicate that doping with an appropriate amount of V-ion can improve the electrochemical activity of $LiFePO_4$/C composite.

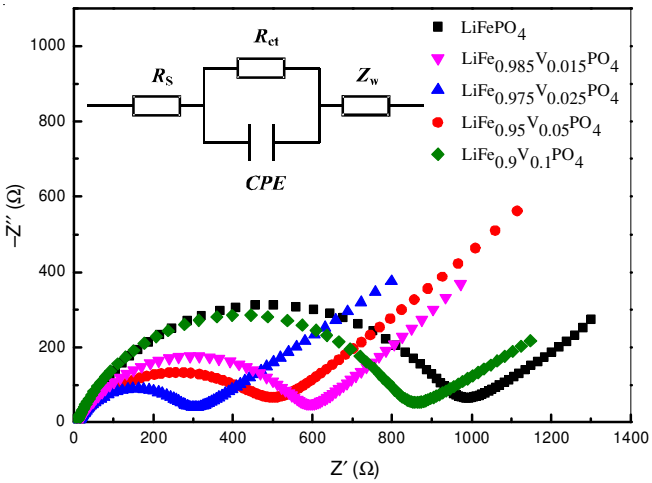

Fig. 8. Electrochemical impedance spectra profile of samples and equivalent circuit

Conclusion

$LiFePO_4$/C doped with different vanadium content is successfully synthesized by the carbothermal reduction method. The XRD results indicate that only a little of vanadium substitutes the iron into the crystal lattice and the impurity phase exists when the vanadium content is over 0.5 mol %. The formation of impurity phase, $LiVOPO_4$ or $Li_3V_2(PO_4)_3$, depends on the doping level and has a dramatic effect on electrochemical performance. The valences of vanadium in $LiFe_{0.975}V_{0.025}PO_4$/C and $LiFe_{0.9}V_{0.1}PO_4$/C are both between 3^+-4^+, according to the XPS result. $LiFePO_4$/C doped with 2.5 mol % vanadium not only shows the best special capacity and rate capability, but also has higher ionic conductivity and reversibility of redox reaction, owing to the presence of $LiVOPO_4$. Therefore, the enhancement of the electrochemical performance should be mainly due to the existence of a small amount of impurity phase, especially $LiVOPO_4$, rather than the doping of vanadium in the host lattice.

ACKNOWLEDGEMENTS

The authors are grateful for the financial support from the Natural Science Foundation of Hebei Province (B2012203069) and support from Education Department of Hebei Province on Natural Science Research Key Projects for Institution of Higher Learning (ZH2011228).

REFERENCES

1. M.X. Gao, Y. Lin, Y.H. Yin, Y.F. Liu and H.G. Pan, *Electrochim. Acta*, **55**, 8043 (2010).
2. Y. Liu, C.H. Mi, C.Z. Yuan and X.G. Zhang, *J. Electroanal. Chem.*, **628**, 73 (2009).
3. C. Delacourt, P. Poizot, S. Levasseur and C. Masquelier, *Electrochem. Solid-State Lett.*, **9**, A352 (2006).
4. G.T. Fey, Y.G. Chen and H.M. Kao, *J. Power Sources*, **189**, 169 (2009).
5. M. Wagemaker, B.L. Ellis, D. Lützenkirchen-Hecht, F.M. Mulder and L.F. Nazar, *Chem. Mater.*, **20**, 6313 (2008).
6. Y.C. Ge, X.D. Yan, J. Liu, X.F. Zhang, J.W. Wang, X.G. He, R.S. Wang and H.M. Xie, *Electrochim. Acta*, **55**, 5886 (2010).
7. J.W. Yao, F. Wu, X.P. Qiu, N. Li and Y. Su, *Electrochim. Acta*, **56**, 5587 (2011).
8. Y. Yang, X.Z. Liao, Z.F. Ma, B.F. Wang, L. He and Y.S. He, *Electrochem. Commun.*, **11**, 1277 (2009).

9. C.S. Sun, Z. Zhou, Z.G. Xu, D.G. Wang, J.P. Wei, X.K. Bian and J. Yan, *J. Power Sources*, **193**, 841 (2009).
10. J. Hong, C.S. Wang, X. Chen, S. Upreti and M.S. Whittingham, *Electrochem. Solid-State Lett*., **12**, A33 (2009).
11. J.S. Sakamoto and B. Dunn, *J. Mater. Chem*., **12**, 2859 (2002).
12. J. Ma, B.H. Li, H.D. Du, C.J. Xu and F.Y. Kang, *J. Electrochem. Soc*., **158**, A26 (2011).
13. Y. Jin, C.P. Yang, X.H. Rui, T. Cheng and C.H. Chen, *J. Power Sources*, **196**, 5623 (2011).
14. J. Barker, M.Y. Saidi, R.K.B. Gover, P. Burns and A. Bryan, *J. Power Sources*, **174**, 927 (2007).
15. M.M. Ren, Z. Zhou, X.P. Gao, L. Liu and W.X. Peng, *J. Phys. Chem. C*, **112**, 13043 (2008).
16. F. Omenya, N.A. Chernova, S. Upreti, P.Y. Zavalij, K.W. Nam, X.Q. Yang and M.S. Whittingham, *Chem. Mater*., **23**, 4733 (2011).
17. L.L. Zhang, G. Liang, A. Ignatov, M.C. Croft, X.Q. Xiong, M. Hung, Y.H. Huang, X.L. Hu, W.X. Zhang and Y.L. Peng, *J. Phys. Chem. C*, **115**, 13520 (2011).
18. H.T. Kuo, N.C. Bagkar, R.S. Liu, C.H. Shen, D.S. Shy, X.K. Xing, J.F. Lee and J.M. Chen, *J. Phys. Chem. B*, **112**, 11250 (2008).
19. J.M. Tarascon and M. Armand, *Nature*, **414**, 359 (2001).
20. W.J. Zhang, *J. Power Sources*, **196**, 2962 (2011).
21. G.X. Wang, L. Yang, Y. Chen, Z. Wang, S. Bewlay and H.K. Liu, *Electrochim. Acta*, **50**, 4649 (2005).
22. J.L. Liu, R.R. Jiang, X.Y. Wang, T. Huang and A.S. Yu, *J. Power Sources*, **194**, 536 (2009).